# Cavity Catalysis
# –Accelerating Reactions under Vibrational Strong Coupling–

Hidefumi Hiura[1*], Atef Shalabney[2], Jino George[3]

[1]System Platform Research Laboratories, NEC Corporation,
4 Miyukigaoka, Tsukuba 305-8501, Japan.

[2]Physics and Optical Engineering Department, Braude College,
Snunit St 51, Karmiel, 2161002, Israel.

[3]Department of Chemical Sciences, Indian Institute of Science Education and Research (IISER) Mohali,
Punjab-140306, India.

*Correspondence to: h-hiura@bq.jp.nec.com

**Abstract**

In conventional catalysis the reactants interact with specific sites of the catalyst in such a way that the reaction barrier is lowered and the reaction rate is accelerated. Here we take a radically different approach to catalysis by strongly coupling the vibrations of the reactants to the vacuum electromagnetic field of a cavity. To demonstrate the possibility of such cavity catalysis, we have studied hydrolysis reactions under strong coupling of the OH stretching mode of water to a Fabry-Pérot (FP) microfluidic cavity mode. This results in an exceptionally large Rabi splitting energy $\hbar\Omega_R$ of 92 meV (740 $cm^{-1}$), indicating the system is in vibrational ultra-strong coupling (V-USC) regime and we have found that it enhances the hydrolysis reaction rate of cyanate ions by $10^2$ times and that of ammonia borane by $10^4$ times. This catalytic ability is shown to depend only upon the cavity tuning and the coupling ratio. Given the vital importance of water for life and human activities, we expect our finding not only offers an unconventional way of controlling chemical reactions by ultra-strong light-matter interactions, but also changes the landscape of chemistry in a fundamental way.

## Introduction

Over the past quarter of a century, strong and ultra-strong coupling between light and matter has been realized for a number of physical systems and used to create novel states and properties. Such light-matter interactions have recently opened up an intriguing frontier for material science and chemistry (*1*). In particular, it has been demonstrated that chemical reactions can be modified by coupling either the reactant's electronic or vibrational transitions (*2*, *3*). In the latter case, a vibrational mode of a molecule is resonantly coupled to an optical mode of a cavity thereby creating a pair of vibro-polaritonic states, *i.e.*, light-matter hybrid states (*1, 4*) (Fig. 1). Such vibrational strong coupling, or V-SC with vacuum field (zero-point energy of the cavity as discussed below) has been demonstrated both for solids and liquids in FP cavities (*1, 3, 5–14*). Moreover, theoretical light-matter interaction systems have been studied to try to understand how electronic strong and ultra-strong coupling affect the chemical properties of the systems (*15−17*).

In sharp contrast to earlier studies where the reaction rates decreased under strong coupling (*3*), here we demonstrate for the first time a cavity catalysis based on V-SC and vibrational ultra-strong coupling V-USC. We first analyze the IR spectroscopic features of vibro-polaritonic states that are formed by coupling the OH stretching mode of water with the vacuum field of a micro-fluidic FP cavity and compare that to the case for OD mode of $D_2O$. We then show that the rate of a chemical reaction can be boosted up to two to four orders of magnitude using water under V-USC.

## Results & Discussions

Figure 1 schematically outlines the vibrational light-matter coupling of water to an FP cavity. In brief, as shown in column (b) with rows from (i) to (iii), a pair of polaritonic states ($P_-$ and $P_+$) appears when the OH stretch mode of water is vibrationally coupled with a given optical mode of an FP cavity under the resonant condition of $\omega_0 = \omega_c$, where $\omega_0$ is the fundamental vibrational frequency of the OH stretch mode and $\omega_c$ is the frequency of a cavity mode. The difference in energy between $P_+$ and $P_-$, the so-called Rabi splitting energy $\hbar\Omega_R$ is generally given by the following relations (*1, 4, 7*):

$$\begin{aligned}\hbar\Omega_R &= 2\sqrt{N}Ed\sqrt{n_{ph}+1} \\ &= 2\sqrt{N}\sqrt{\frac{\hbar\omega_0}{2\varepsilon_0 V}}d\sqrt{n_{ph}+1}\end{aligned} \quad (1)$$

where $\hbar$ is the reduced Planck constant, $N$ is the number of coupled molecules, $E$ is the amplitude of the electric field of light, $d$ is the transition dipole moment of the molecules, $n_{ph}$ is the number of photons populating the cavity mode, $\varepsilon_0$ is the dielectric constant of vacuum, and $V$ is the mode volume. When $n_{ph}$ is zero, $\hbar\Omega_R$ has a residual value which is known as the vacuum Rabi splitting which is due to the vacuum field (the zero point energy of the cavity mode). The coupling ratio or the coupling strength is defined as half of the ratio of the vacuum Rabi splitting frequency to the fundamental transition frequency of the molecules (*18, 19*); that is, $\Omega_R/2\omega_0$. The boundary between the strong and ultra-strong coupling regimes is most often drawn at $\Omega_R/2\omega_0 = 0.1$ (*18–20*). Note that $\Omega_R/2\omega_0$ is a crucial factor to determine the catalytic power for cavity catalysis under V-SC as shown later.

To achieve strong coupling, the FP cavity is tuned to a vibrational mode of the molecule by simply adjusting the distance between the two mirrors of the cavity (see Supporting Information (3)). Figures 2A and 2B compare the IR transmission spectra of light-coupled OH (OD) oscillators in $H_2O$ ($D_2O$) water at various concentrations obtained by diluting $H_2O$ ($D_2O$) with $D_2O$ ($H_2O$). The original OH and OD modes

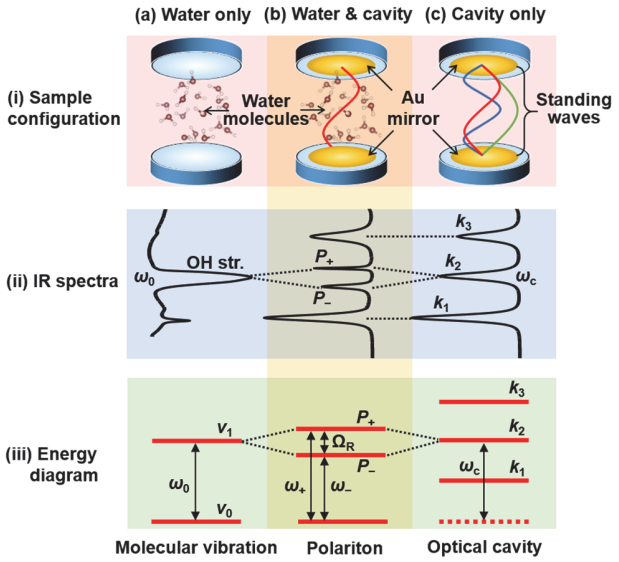


**Fig. 1. Schematic overview of the vibrational light-matter coupling.** The top, middle and bottom rows show (i) experimental configurations, (ii) infrared transmission spectra and (iii) energy diagrams. The left, middle and right columns correspond to (a) water not in an FP cavity, (b) water in an FP cavity and (c) an FP cavity without water.

are located at 3400 $cm^{-1}$and 2500 $cm^{-1}$, respectively. These modes are coupled to the 9th and 7th cavity modes, thereby forming pairs of vibro-polaritonic states $P_{9+}/P_{9-}$ and $P_{7+}/P_{7-}$, respectively. The measured $\Omega_R$ is approximately 740 $cm^{-1}$ for pure $H_2O$ and 540 $cm^{-1}$ for pure $D_2O$. As shown by the dotted lines in Figs. 2A and 2B, $\Omega_R$ decreases as $C$ decreases. The square root dependence is expected from Eq. (1), namely, $\Omega_R/2\omega_0 = A_c(C/C_0)^{0.5}$ where $A_c$ is a constant equal to $\Omega_R/2\omega_0$ of the pure material. The least-squares fits give $A_c = 0.113$ for $H_2O$ and 0.111 for $D_2O$, confirming that the vibrational strong coupling of pure water occur in the ultra-strong coupling regime as discussed above. Note that light-coupled water has one of the largest $\Omega_R/2\omega_0$ ever reported for V-SC and V-USC (*8*).

Next the hydrolysis reaction under V-USC of the OH (OD) stretching mode for the following reaction is studied:

$$2H_2O\ (2D_2O) + OCN^- \rightarrow CO_3^{2-} + NH_4^+\ (ND_4^+)$$

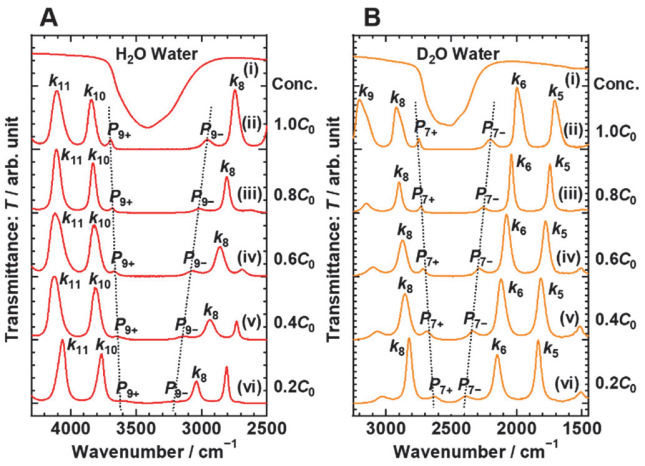


**Fig. 2. Experimental results of light-coupled OH (OD) oscillators in water and related compounds.** (A, B) Comparison of IR transmission spectra of light-coupled $H_2O$ ($D_2O$) at various concentrations. (i) is the IR spectrum of pure $H_2O$ ($D_2O$) in an IR cell, whereas each spectrum from (ii) to (vi) was measured with an FP cavity when the concentration of $H_2O$ ($D_2O$) was reduced in decrements of $0.2C_0$. All the spectra are normalized to unity.

where $H_2O$ ($D_2O$) act both as the reactant and the solvent for the hydrolysis of cyanate ions ($OCN^-$). Figures 3A and 3B present the comparisons of temporal changes in IR spectra observed for the hydrolysis of $OCN^-$ in uncoupled $H_2O$ ($D_2O$) and under V-USC at room temperature (see Supporting Information (4) for details). The insets of Figs. 3A and 3B show that the absorption band of $OCN^-$ stretch decreases much faster under V-USC of the water OH (OD) stretching mode. Since water was present in a large excess over $OCN^-$ in these solutions, the hydrolysis obeys a pseudo-first-order rate equation, $C = C_0 \exp(-\kappa' t)$, where $C$ is the time-dependent concentration of $OCN^-$, $C_0$ is the initial concentration of $OCN^-$ (2.00 mol·dm$^{-3}$), $\kappa'$ is the observed reaction rate constant of the hydrolysis (*i.e.* the product of the absolute rate constant $\kappa$ and the $H_2O$ ($D_2O$) concentration), and $t$ is the reaction time. Thus from the logarithmic plot, the rate constants can be extracted from the slopes, giving a rate constant under V-USC of $H_2O$ ($D_2O$), $\kappa'_{\text{V-USC}} = 6.4 \times 10^{-5}$ ($1.6 \times 10^{-5}$) s$^{-1}$, while that for the uncoupled $H_2O$ ($D_2O$) is $\kappa'_0 = 5.6 \times 10^{-7}$ ($5.1 \times 10^{-7}$) s$^{-1}$, demonstrating a 100 fold enhancement in the

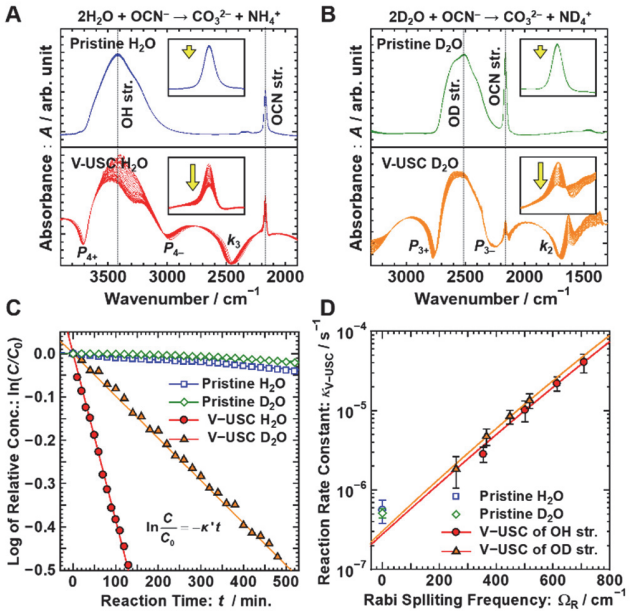


**Fig. 3. Demonstration of the cavity catalyst under V-USC of water.** (A and B) Comparison of temporal changes in IR absorption spectra observed for the hydrolysis of $OCN^-$ with pristine and V-USC $H_2O$ water (upper left), and pristine and V-USC $D_2O$ water (upper right). Insets show the magnified O=C=N stretch band during the reaction. (C) Comparison of the reaction profile for the hydrolysis of $OCN^-$. (D) $\kappa'_{\text{V-USC}}$ *vs.* $\Omega_R$ on a semi-logarithm scale for light-coupled OH and OD oscillators. Each bar denotes the standard errors of experimental values. The curves were drawn according to Eq. (2) by least-squares fitting. As a guide, $\kappa_0$ of pristine $H_2O$ ($5.61 \pm 1.82 \times 10^{-7}$ s$^{-1}$) and $D_2O$ ($5.12 \pm 0.68 \times 10^{-7}$ s$^{-1}$) were respectively plotted at $\Omega_R = 0$ cm$^{-1}$.

absolute rate constant under V-USC for $H_2O$ and a 30 fold enhancement for $D_2O$. We attribute the above double-digit acceleration to the reduction in activation energy under V-USC: a quantitative estimate based on the Arrhenius equation yields about an 18 % reduction in activation energy if $\kappa'_{\text{V-USC}}/\kappa_0 = 114$ (see Supporting Information (6) with eq. (S4)). This observed reduction agrees well with a theoretical value of 20 % which is predicted according to Eq. (2) (*vide infra*). Figure 3D shows the dependence of $\kappa'_{\text{V-USC}}$ *vs.* coupling strength $\Omega_R$ for light-coupled OH (OD) oscillators was tuned from 709 (518) to 355 (259) cm$^{-1}$ by diluting $H_2O$ ($D_2O$) with $D_2O$ ($H_2O$). $\kappa'_{\text{V-USC}}$ increases exponentially with an increase of $\Omega_R$ for both OH and OD coupled vibrations.

Next, we attempt to understand these results in terms of transition state theory. The splitting of the first vibrational level ($v$ = 1, Fig. 1) will most likely change the force constant $k$ of the vibrational mode since $\omega_0$ is proportional to square root of $k$ ($\omega_0 \propto \sqrt{k}$) and since reactivity often correlates with $k$ (*21*), we can assume for the purposes of this discussion that it lowers the reaction barrier. Such qualitative picture of the cavity catalysis can be analytically described by using the relative reaction rate constant $\kappa_-/\kappa_0$ as a measure as follows: by substituting next two formulae, $\omega_-/\omega_0 = (1 - \Omega_R/2\omega_0)$ and $E_{V\text{-}SC}/E_0 = (1 - \Omega_R/2\omega_0)^2$ where $E_{V\text{-}SC}$ is the activation energy under V-SC and $E_0$ is the original activation energy, into the Eyring–Polanyi equation of the transition state theory (*21*, *22*), we obtain the following equation (*23*):

$$\frac{\kappa_{V\text{-}SC}}{\kappa_0} = \left(1 - \frac{1}{2}\frac{\Omega_R}{\omega_0}\right) \times \exp\left[\left(-\frac{E_0}{k_B T}\right)\left\{\left(1 - \frac{1}{2}\frac{\Omega_R}{\omega_0}\right)^2 - 1\right\}\right] \quad (2)$$

where $\kappa_{V\text{-}SC}$ is the reaction rate constant under V-SC, $\kappa_0$ is the reaction rate constant of the original reaction, $k_B$ is Boltzmann constant, and $T$ is the absolute temperature. Equation (2) is a function of $\Omega_R/2\omega_0$, indicating that $\Omega_R/2\omega_0$ or $\Omega_R$ is a key parameter for cavity catalysis as mentioned earlier. As $\Omega_R/2\omega_0$ increases, $\kappa_{V\text{-}SC}/\kappa_0$ decreases exponentially. Note that the relation between $\kappa'_{V\text{-}USC}$ and $\Omega_R$ for both light-coupled OH and OD oscillators (Fig. 3D) can be well fitted by Eq. (2) (see Supporting Information (4) with eq. (S2)). For example, when inputting $\kappa'_{V\text{-}USC}$ and $\Omega_R$ as variables together with $T$ = 300 K and $\omega_0$ = 3400 $cm^{-1}$ for OH oscillators as a fixed value into Eq. (2), we extracted $E_0$ = 15.3 kcal·mol$^{-1}$ (0.66 eV) by the least-squares fitting. The obtained $E_0$ is in a good agreement with the literature value of 16 kcal·mol$^{-1}$ (0.69 eV) (*24*). As the data and Eq. (2) show, the larger $\Omega_R/2\omega_0$ or $\Omega_R$ is preferable to obtain a larger catalytic effect in the cavity. Hence, water can be considered as a prime candidate for cavity catalysis.

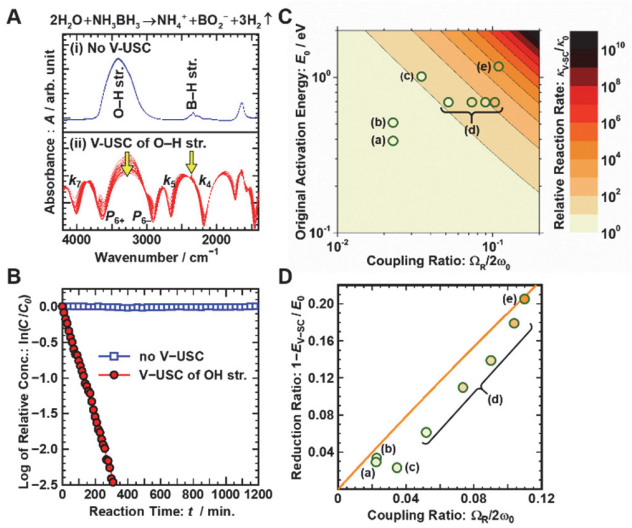


**Fig.4. Comparison of cavity-catalyzed reactions under V-SC and V-USC.** (A) Comparison of temporal changes of IR spectra observed for a hydrolysis of $NH_3BH_3$, (i) without V-USC, and (ii) with V-USC of the O–H stretch. (B) Comparison of reaction profiles under the conditions of (i) and (ii). The rate constants were determined assuming a pseudo-first-order rate reaction as follows: (i) $\kappa'_0$ = 1.289 × 10$^{-8}$ s$^{-1}$ (blue), and (ii) $\kappa'_{V\text{-}USC}$ = 1.287 × 10$^{-4}$ s$^{-1}$ (red). (C) Color plots of $\kappa_{V\text{-}SC}/\kappa_0$ as functions of $E_0$ and $\Omega_R/2\omega_0$ at $T$ = 300K calculated by Eq. (2) with superimposing the data points observed for the cavity-catalyzed reactions: (a) V-SC of N=C=O str. (methanol), (b) V-SC of N=C=O str. (2-propanol), (c) V-SC of O=C=N str. ($NH_4^+$), (d) V-SC and V-USC of O–H str. ($OCN^-$), (e) V-USC of O–H str. ($NH_3BH_3$). (D) $1-E_{V\text{-}SC}/E_0$ *vs.* $\Omega_R/2\omega_0$. (a) to (e) correspond to the same cavity-catalyzed reactions as those in Fig. 4C. The detail of the data points for (a) to (e) in Fig. 4C and 4D is summarized in table S1.

In the next example, a ten-thousand-fold acceleration in the hydrolytic dehydrogenation of ammonia borane ($NH_3BH_3$) under V-USC of $H_2O$ was observed as shown in Figs. 4A and 4B (see Supporting Information (5) for details). Equation (2) predicts exactly $\kappa_{V\text{-}SC}/\kappa_0 = \sim 10^4$ for this hydrolysis. In contrast to such large chemical boosts under V-USC of water, non-aqueous cavity-catalyzed reactions exhibit less than three times promotion in the reaction rate (see Supporting Information (7) to (11) with figs. S1 to S5). The main reason for such insufficient acceleration is that it is very difficult to provide V-USC conditions for vibro-polaritons of non-aqueous reactants in solutions.

All the cavity-catalyzed reactions are further evaluated in a quantitative manner from a viewpoint of how $\Omega_R/2\omega_0$ and $E_0$ affect $\kappa_{V\text{-}SC}/\kappa_0$. Figures 4C compares the calculated and observed $\kappa_{V\text{-}SC}/\kappa_0$ as functions of $\Omega_R/2\omega_0$ and $E_0$ at room temperature: the calculated color plot shows to what extent the cavity catalyst accelerates reactions on the basis of Eq. (2), while the data points (a) to (e) drawn in green are extracted from the reaction profiles of the cavity-catalyzed reactions in this study (table S1). For the data point (c), the calculated $\kappa_{V\text{-}SC}/\kappa_0$ differs from the observed one by half an order of magnitude, however, the other data points fit well with the calculated color plots in that the deviation is no more than a factor of about two over a wide range of $\kappa_{V\text{-}SC}/\kappa_0$ up to $10^4$. We thus conclude that overall, Eq. (2) can rather well predict the observed trends of the cavity catalysis. Figure 4D manifests this conclusion more clearly: the reduction ratio in activation energy by V-SC, $1-E_{V\text{-}SC}/E_0$, which is obtained on the basis of the Arrhenius equation (eq. (S4)), increases from 2% to over 20 % with an increase of $\Omega_R/2\omega_0$ from 0.02 to 0.11. This tendency is reproduced by the theoretical curve based on Eq. (2). More importantly, these results clarify that the cavity catalysis indeed lowers the activation energy depending on the strength of $\Omega_R/2\omega_0$. Nonetheless, considering the myriad of chemical reactions and their diverse nature, it will be necessary to compare more examples of different types of reactions under V-SC and V-USC in order to understand how the cavity catalysis works.

It is clear that water fills a special niche in cavity catalysis reported here: water can serve not only as highly catalytic vibro-polaritons but also as a reaction solvent, that is, V-USC water can keep high reactivity all the way to the endpoint of reactions since it is not depleted. Moreover, water is of the essence in nature and in industry in that they utilize water as reactant and media for numerous chemical reactions. We thus expect that V-USC of water can play a central role for cavity catalysis.

**References**


1. T.W. Ebbesen, Hybrid light-matter states in a molecular and material science perspective. *Acc. Chem. Res.* **49**, 2403-2412 (2016).
2. J. A. Hutchison, T. Schwartz, C. Genet, E. Devaux, T. W. Ebbesen, Modifying chemical landscapes by coupling to vacuum fields. *Angew. Chem. Int. Ed*. **51**, 1592−1596 (2012).
3. A. Thomas, J. George, A. Shalabney, M. Dryzhakov, S. J. Varma, J. Moran, T. Chervy, X. Zhong, E. Devaux, C. Genet, J. A. Hutchison, T.W. Ebbesen, Ground-state chemical reactivity under vibrational coupling to the vacuum electromagnetic field. *Angew. Chem. Int. Ed*. **55**, 1−6 (2016).
4. P. Törmä, W. L. Barnes, Strong coupling between surface plasmon polaritons and emitters: a review. *Rep. Prog. Phys*. **78**, 013901(34) (2014).
5. A. Shalabney, J. George, J. Hutchison, G. Pupillo, C. Genet, T.W. Ebbesen, Coherent coupling of molecular resonators with a microcavity mode. *Nat. Comm*. **6**, 5981(6) (2015).
6. A. Shalabney, J. George, H. Hiura, J. A. Hutchison, C. Genet, P. Hellwig, T.W. Ebbesen, Enhanced Raman scattering from vibro-polariton hybrid states. *Angew. Chem. Int. Ed*. **54**, 7971−7975 (2015).
7. J. George, A. Shalabney, J. A. Hutchison, C. Genet, T.W. Ebbesen, Liquid-phase vibrational strong coupling. *J. Phys. Chem. Lett*. **6**, 1027−1031 (2015).
8. J. George, T. Chervy, A. Shalabney, E. Devaux, H. Hiura, C. Genet, T.W. Ebbesen, Multiple Rabi splittings under ultrastrong vibrational coupling. *Phys. Rev. Lett*. **117**, 153601(5) (2016).

9. J. P. Long, B. S. Simpkins, Coherent coupling between a molecular vibration and Fabry–Pérot optical cavity to give hybridized states in the strong coupling limit. *ACS Photonics* ***2*** **(1)**, 130-136 (2015).

10. A. D. Dunkelberger, B. T. Spann, K. P. Fears, B. S. Simpkins, J. C. Owrutsky, Modified relaxation dynamics and coherent energy exchange in coupled vibration-cavity polaritons. *Nat. Comm.* **7**, 13504(10) (2016).

*11.* B. Xiang, R. F. Ribeiro, A. D. Dunkelberger, J. Wang, Y. Lia, B. S. Simpkins, J. C. Owrutsky, J. Yuen-Zhou, W. Xiong, Two-dimensional infrared spectroscopy of vibrational polaritons. *Proc. Natl. Acad. Sci. USA* **115**, 4845-4850 (2018).

12. M. Hertzog, P. Rudquist, J. A. Hutchison, J. George, T.W. Ebbesen, K. Börjesson, Voltage–controlled switching of strong light–matter interactions using liquid crystals. *Chem. Eur. J.* ***23***, 18166 (2017).

13. R. M. A. Vergauwe, J. George, T. Chervy, J. A. Hutchison, A. Shalabney, V. Y. Torbeev, T.W. Ebbesen, Quantum strong coupling with protein vibrational modes. *J. Phys. Chem. Lett*. **7**, 4159−4167 (2016).

14. V. F. Crum, S. R. Casey, J. R. Sparks, Photon-mediated hybridization of molecular vibrational states. *Phys. Chem. Chem. Phys.* **20**, 850–857 (2018).

15. F. Herrera, F. C. Spano, Cavity-controlled chemistry in molecular ensembles. *Phys. Rev. Lett.* **116**, 238301(6) (2016).

16. J. Flick, M. Ruggenthaler, H. Appel, A. Rubio, Atoms and molecules in cavities, from weak to strong coupling in quantum-electrodynamics (QED) chemistry. *Proc. Natl. Acad. Sci. USA* **114**, 3026−3034 (2017).

17. L. A. Martínez-Martínez, R. F. Ribeiro, J. Campos-González-Angulo, J. Yuen-Zhou, Can ultrastrong coupling change ground-state chemical reactions? *ACS Photonics* **5**, 167−176 (2018).

18. C. Ciuti, G. Bastard, Quantum vacuum properties of the intersubband cavity polariton field. *Phys. Rev. B* **72**, 115303(9) (2005).

19. S. J. Bosman, M. F. Gely, V. Singh, A. Bruno, D. Bothner, G. A. Steele, Multi-mode ultra-strong coupling in circuit quantum electrodynamics. *npj Quantum Information* **3**, 46(6) (2017).

20. J. Casanova, G. Romero, I. Lizuain, J. J. García-Ripoll, E. Solano. Deep strong coupling regime of the Jaynes-Cummings model. *Phys. Rev. Lett*. **105**, 263603(4) (2010).

21. H. Eyring, The activated complex in chemical reactions. *J. Chem. Phys*. **3**, 107 (1935).

22. P. Hänggi, P. Talkner, Reaction-rate theory: fifty years after Kramers. *Rev. Mod. Phys*. **62(2)**, 251–341 (1990).

23. H. Hiura, Vibrational ultra-strong coupling between light and molecules, and its application to chemistry. *Bull. Solid State Phys. Appl.* **24(1)**, 9–14 (2018).

24. M. W. Lister, Some observations on cyanic acid and cyanates. *Can. J. Chem*. **33**, 426–440 (1955).

**Acknowledgments**

H.H. thanks Professor Thomas W. Ebbesen for teaching the fundamentals of V-SC and V-USC. H.H. also thanks Jingwen Lu for assisting in the laboratory work.

**Author contributions**

A.S. and J.G instructed H.H in the experimental techniques of V-SC and V-USC. H.H planed the project of the cavity catalysis under V-USC of water. H.H acquired and analyzed the IR data. H.H wrote the manuscript and A.S and J.G revised it. All authors contributed to discussions.